Proceedings of the 9th U.S. National and 10th Canadian Conference on Earthquake Engineering
Compte Rendu de la 9ième Conférence Nationale Américaine et
10ième Conférence Canadienne de Génie Parasismique
July 25-29, 2010, Toronto, Ontario, Canada • Paper No 939

EXPERIMENTAL EVALUATION OF STEEL MRF PERFORMANCE WITH LARGE SCALE PASSIVE MAGNETO-RHEOLOGICAL DAMPERS FOR SEISMIC HAZARD MITIGATION USING REAL-TIME HYBRID SIMULATION

Cheng Chen[1], James M. Ricles[2], Richard Sause[3] and Theodore L. Karavasilis[4]

ABSTRACT

Magneto-Rheological (MR) fluid dampers are a means to achieve seismic hazard mitigation of civil engineering structures. Validation studies require large- or full-scale real-time testing in order to take into account rate dependent behavior of the damper. Real-time hybrid simulation combines physical testing and numerical simulation so that the dynamic performance of a structural system can be considered in a realistic and efficient manner. In this paper the experimental evaluation of large scale MR fluid dampers for seismic hazard mitigation in buildings is presented through real-time hybrid simulation. A simplified design procedure is applied to design a two-story, four-bay steel moment resisting frame (MRF) prototype structure with MR fluid dampers in passive mode. The steel MRF is modeled analytically by a finite element program and the MR fluid dampers are modeled as experimental substructures. The unconditionally stable explicit CR integration algorithm and an adaptive inverse compensation scheme are used for structural response calculation and minimizing actuator delay, respectively. Real-time hybrid simulations were conducted using ten different ground motions to statistically evaluate the performance of the MRF design. The simulation results show that the simplified design procedure enables an efficient design to be achieved for an MRF with MR fluid dampers in passive mode. The real-time hybrid simulation method using the CR algorithm and the adaptive inverse compensation demonstrates great potential for structural research on developing performance-based design procedures for structures with rate-dependent devices.

Introduction

Passive energy dissipating devices have shown great potential for seismic hazard mitigation of civil engineering structures due to their attractive properties such as little or no power requirements. Previous research has shown that passive dampers can significantly enhance structural performance by reducing inelastic deformation demands on the primary lateral load resisting system and the drift, acceleration and velocity demands on non-structural components [Soong and Dargush 1997]. Modern building design provisions [BSSC 2003] permit the structural engineer to utilize passive devices to attain better or similar performance as that of conventional lateral load resisting systems. A Magneto-Rheological (MR) fluid damper is an energy dissipating device whose characteristics can be changed by varying the magnetic field in the device through different current inputs. In addition to its small power requirement, MR fluid

[1]Assistant Professor, School of Engineering, San Francisco State University, San Francisco, CA 94132
[2] Bruce. G. Johnston Professor, ATLSS Engineering Research Center, Lehigh University, Bethlehem, PA, 18015
[3] Joseph T. Stuart Professor, ATLSS Engineering Research Center, Lehigh University, Bethlehem, PA, 18015
[4] Research Associate, ATLSS Engineering Research Center, Lehigh University, Bethlehem, PA, 18015

dampers can generate large forces at low velocities. It therefore offers a great potential for seismic hazard mitigation of building structures. Successful application of MR fluid dampers for seismic hazard mitigation requires that their behavior be well understood and the design procedure be experimentally validated. Moreover, the rate-dependency of MR fluid damper requires real-time experiments to acquire accurate and reliable results.

Various testing techniques have been developed for structural engineering research, including: quasi-static cyclic testing; shake-table testing; pseudodynamic testing; and hybrid simulation. Although shake-table testing provides the most realistic means of simulating seismic effects, the test structure is usually a scaled-down version of the prototype structure in order to accommodate the capacity of the shake table. Due to the scaling effect, shake-table tests of reduced-scale models may not accurately replicate the behavior of some full scale energy dissipation devices. Real-time hybrid simulation is a newly developed experiment technique [Nakashima *et al.* 1992; Blakeborough *et al.* 2001; Bonnet *et al.* 2007]. It divides the structure into analytical and experimental substructures. By numerically modeling parts of the structural system using the finite element method and physically testing the experimental substructures in the laboratory, real-time hybrid simulation provides a viable technique to experimentally evaluate the performance of large- or full-scale structural systems. The interaction between the integration algorithm and the substructures ensures that the dynamic performance of the entire structural system is considered throughout the simulation. Real-time hybrid simulation is especially efficient for the experimental evaluation of the performance of structural steel systems with rate-dependent devices, where the latter are often tested as experimental substructures and the steel structure is modeled analytically. Experiments on MR fluid dampers have been reported by numerous researchers [Dyke *et al.* 1998; Yang *et al.* 2002] to develop numerical models and semi-active control strategies. More recently, large-scale real-time hybrid simulation of MR fluid dampers was reported by Christenson *et al.* [2008] for a semi-actively controlled building. In this paper the performance of MR fluid dampers for seismic hazard mitigation of steel MRF structures is evaluated for a number of selected ground motions scaled to the design basis earthquake (DBE). A simplified design procedure is used to design a two-story four-bay MRF with MR fluid dampers in passive mode (i.e., with constant current input field). The performance of the resulting MRF is experimentally evaluated through real-time hybrid simulation.

Prototype Steel Moment Resisting Frame

A 2-story, 6-bay by 6-bay office building is selected as the prototype structure for the experimental study reported in this paper. The office building is assumed to be located on stiff soil site near Los Angeles and has four identical perimeter steel MRFs to resist lateral forces. Fig. 1 shows the plan view and the perimeter frame of the prototype structure. The experimental study presented in this paper focuses on one typical perimeter MRF, which is designed with MR fluid dampers as shown in Fig. 1(b). The yield strength of the material for the MRF is assumed to be equal to 345 MPa. The gravity loads described in the International Building Code [ICC 2006] are considered in the design. A smooth design response spectrum with parameters S_{DS}=1.0, S_{D1}=0.6, T_0=0.12 sec. and T_s=0.6 sec. represents the design basis earthquake (DBE) [BSSC 2003].

A simplified design procedure developed by Lee *et al.* [2005] is used to design the MRF

with MR fluid dampers in passive mode, where the properties of the resulting MRF are tabulated in Table 1, including column and beam cross-sections, fundamental period of vibration and story stiffness. The MR fluid dampers are assumed to be in passive mode with a current input of 2.5 Amps. A design base shear equal to 50% of that of a conventional SMRF is used to design the MRF,. The number of MR fluid dampers is determined by the simplified design procedure to be six and four for the first and second stories, respectively, in order to achieve a performance having a maximum story drift of 1.7% under the design basis earthquake [Chen *et al.* 2009a].

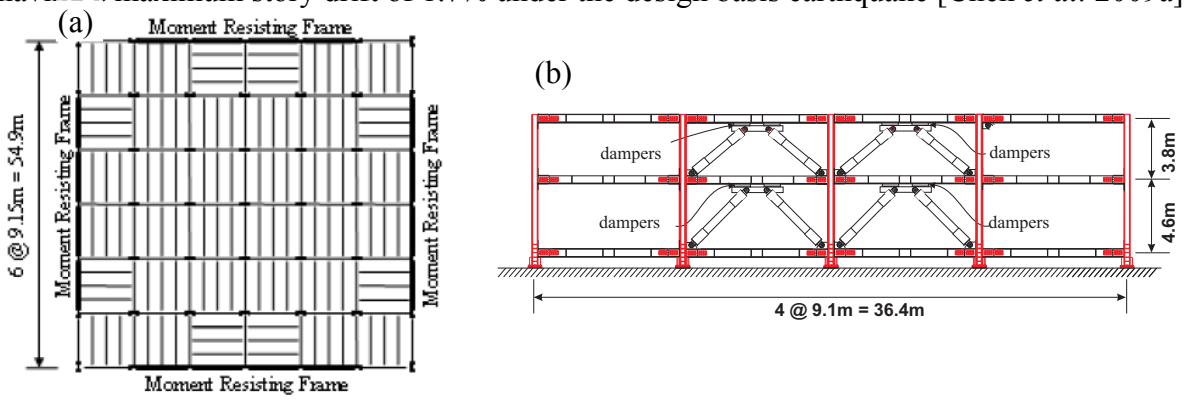

Figure 1. Prototype building (a) plan view; (b) perimeter MRF with dampers and braces

Table 1. Properties of MRF

Column	Beams		T_1 (sec.)	Story Stiffness (kN/m)	
1st and 2nd story	1st story	2nd story	1.42	1st story	2nd story
W14x120	W24x55	W18x40		36007	23894

Experimental Setup for Real-Time Hybrid Simulation

For real-time hybrid simulation, the MR fluid dampers are isolated as the experimental substructures to be physically tested in the laboratory. Since the dampers at a story level of the prototype structure are placed in parallel in the MRF, they are assumed to be subjected to the same velocity and displacement, and hence each of the MR fluid dampers test setups in the laboratory represents all of the dampers in the same story. The measured restoring force from each MR fluid damper setup is multiplied by the number of dampers in the corresponding story of the prototype MRF to obtain the total restoring force of all the dampers at a story level in the MRF. The rest of the structure, i.e., the MRF, is modeled analytically using a nonlinear finite element program with a total 122 degrees of freedom and 71 elements [Karavasilis *et al.* 2009]. Inelastic behavior is modeled by means of a bilinear hysteretic lumped plasticity beam-column element with 3% hardening. In order to overcome the shortcomings of the lumped plasticity model predicting accurately plastic hinge rotation, each physical member (beam or column) was modeled with three beam-column elements in series, i.e., two elements were used to model the two plastic hinge regions at each end of the member with a length equal to 5% of the member length and one element with a length equal to the remaining 90% of the member length.

The real-time hybrid simulation was performed using the NEES Real-Time Multi-Directional (RTMD) Facility at Lehigh University. Fig. 2 shows the experimental setup for the real-time hybrid simulation, which consists of two experimental substructures (two MR fluid

dampers), two servo-hydraulic actuators with supports and roller bearings; reaction frames, and tie-down beams securing the MR fluid dampers to the strong floor. The large-scale MR fluid dampers used in this study are manufactured by Lord Corporation and have a nominal capacity of 200 kN at the current input of 2.5 Amps [Bass and Christenson 2007]. An Advanced Motion Control PWM servo-amplifier is utilized to provide an electrical current command signal that controls the electromagnetic field for the damper. The two actuators in Fig. 2 have the same 500 mm stroke but different force capacities of 1700 kN and 2300 kN. Two servo-valves, each with a flow capacity of 2500 liters/min, are mounted on each of the actuators to enable them to achieve a maximum velocity of 760 mm/sec and 560 mm/sec, respectively. The actuator servo-controller used in the real-time tests consist of a digital PID controller with the proportional gain of 20, integral time constant of 5.0 resulting in an integral gain of 4.0, differential gain of 0 and a roll-off frequency of 39.8 Hz [Lehigh RTMD 2009].

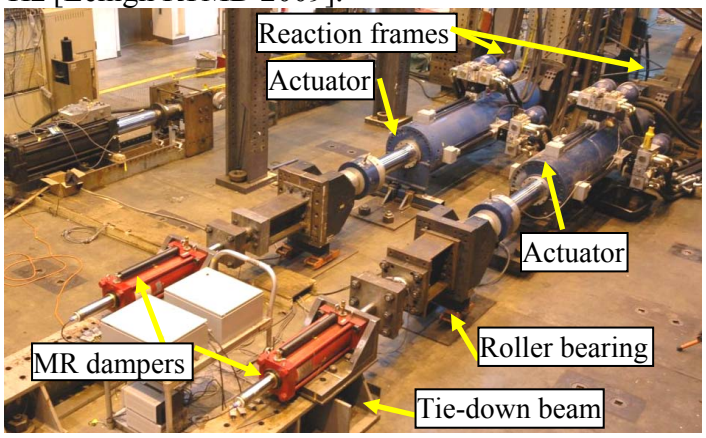

Figure 2. Experimental setup for real-time hybrid simulation

Integration Algorithm and Actuator Delay Compensation

An unconditionally stable explicit integration algorithm [Chen and Ricles 2008a, Chen *et al.* 2009b], referred to as the CR algorithm, is used for the real-time hybrid simulation. For the MRF with MR fluid dampers as shown in Fig. 1, the temporal discretized equations of motion at the i+1th time step can be expressed as

$$\mathbf{M}\cdot\ddot{\mathbf{x}}_{i+1}+\mathbf{C}\cdot\dot{\mathbf{x}}_{i+1}+\mathbf{r}^{a}_{i+1}+\mathbf{r}^{e}_{i+1}=\mathbf{F}_{i+1} \tag{1}$$

where $\ddot{\mathbf{x}}_{i+1}$ and $\dot{\mathbf{x}}_{i+1}$ are the acceleration and velocity vectors of the structure, respectively; $\mathbf{r}^{a}_{i+1}$ and $\mathbf{r}^{e}_{i+1}$ are the restoring force vectors of the analytical and experimental substructures, respectively; **M** and **C** are the mass and damping matrices of the structure, respectively; and $\mathbf{F}_{i+1}$ is the excitation force. The variations of displacement and velocity over the time step are defined as

$$\dot{\mathbf{x}}_{i+1}=\dot{\mathbf{x}}_{i}+\Delta t\cdot\boldsymbol{\alpha}_1\cdot\ddot{\mathbf{x}}_{i} \tag{2a}$$

$$\mathbf{x}_{i+1}=\mathbf{x}_{i}+\Delta t\cdot\dot{\mathbf{x}}_{i}+\Delta t^{2}\cdot\boldsymbol{\alpha}_2\cdot\ddot{\mathbf{x}}_{i} \tag{2b}$$

In Eqs. (2a) and (2b), $\mathbf{x}_i$, $\dot{\mathbf{x}}_i$ and $\ddot{\mathbf{x}}_i$ are the displacement, velocity and acceleration vectors of the MRF structure for the ith time step; $\mathbf{x}_{i+1}$ and $\dot{\mathbf{x}}_{i+1}$ are the displacement and velocity vectors for the (i+1)th time step, respectively; Δt is the integration time step; and $\boldsymbol{\alpha}_1$ and $\boldsymbol{\alpha}_2$ are integration parameter matrices defined as

$$\boldsymbol{\alpha}_1=\boldsymbol{\alpha}_2=4\cdot\left(4\cdot\mathbf{M}+2\cdot\Delta t\cdot(\mathbf{C}+\mathbf{C}_{eq})+\Delta t^{2}\cdot(\mathbf{K}+\mathbf{K}_{eq})\right)^{-1}\cdot\mathbf{M} \tag{3a}$$

In Eq. (3a) **M**, **C** and **K** are the mass, damping and initial linear elastic stiffness matrices of the MRF structure; $\mathbf{K}_{eq}$ and $\mathbf{C}_{eq}$ are matrices that contain terms associated with the equivalent stiffness k_{eq} and the damping c_{eq}, respectively, for the MR fluid dampers. The structural response $\mathbf{x}_{i+1}$ calculated by the CR algorithm is translated into the displacement for the DOFs of the experimental substructures, $\mathbf{x}_{i+1}^{e}$, which is imposed to the MR fluid dampers by the servo-hydraulic actuators. The integration time step Δt used for the present study is equal to 10/1024 sec. To ensure a smooth and continuous actuator response, a ramp generator is used to interpolate the command displacement $\mathbf{x}_{i+1}^{e}$ at the servo controller sampling rate δt, which is equal to 1/1024 sec. For a linear ramp generator, the interpolated command displacement is defined as

$$\mathbf{d}_{i+1}^{c(j)} = \frac{j}{n} \cdot (\mathbf{x}_{i+1}^{e} - \mathbf{x}_{i}^{e}) + \mathbf{x}_{i}^{e} \tag{4}$$

In Eq. (4) $\mathbf{d}_{i+1}^{c(j)}$ is the command displacement vector for the actuators at the jth substep of the (i+1)th time step; $\mathbf{x}_{i}^{e}$ is the command displacement for the experimental substructures at the ith time step; and j is the substep index for the interpolation within one single time step which ranges from 1 to n, where n is the integer ratio of $\Delta t/\delta t$.

Due to the servo-hydraulic dynamics, a time delay will be introduced in response to the displacement command. This time delay is often referred to as actuator delay. Studies by Wallace *et al.* 2005; Chen and Ricles 2008b show that actuator delay can destabilize a real-time hybrid simulation if not compensated properly.An adaptive inverse compensation scheme developed by Chen and Ricles [2009] is used to compensate for actuator delay. The discrete transfer function of the adaptive inverse compensation method is formulated as:

$$G_c(z) = \frac{X^p(z)}{X^c(z)} = \frac{(\alpha_{es} + \Delta\alpha) \cdot z - (\alpha_{es} + \Delta\alpha - 1)}{z} \tag{5}$$

In Eq. (5) α_{es} is the estimated actuator delay; z is the complex variable in the discrete z-domain; and $\Delta\alpha$ is an evolutionary variable with an initial value of zero, and is determined using the following adaptive control law

$$\Delta\alpha(t) = k_p \cdot TI(t) + k_i \cdot \int_0^t TI(\tau)dt \tag{6}$$

In Eq. (6) k_p and k_i are proportional and integrative gains of the adaptive control law, respectively; and TI is the tracking indicator that is formulated for each actuator as [Mercan 2007]

$$TI_{i+1}^{(j)} = 0.5\left(A_{i+1}^{(j)} - TA_{i+1}^{(j)}\right) \tag{7a}$$

$$A_{i+1}^{(j)} = A_{i+1}^{(j-1)} + 0.5\left(d_{i+1}^{c(j)} + d_{i+1}^{c(j-1)}\right)\left(d_{i+1}^{m(j)} - d_{i+1}^{m(j-1)}\right) \tag{7b}$$

$$TA_{i+1}^{(j)} = TA_{i+1}^{(j-1)} + 0.5\left(d_{i+1}^{m(j)} + d_{i+1}^{m(j-1)}\right)\left(d_{i+1}^{c(j)} - d_{i+1}^{c(j-1)}\right) \tag{7c}$$

where $d_{i+1}^{m(j)}$ is the measured displacement for each actuator at the jth substep of the (i+1)th time step. At the beginning of a simulation the tracking indicator has an initial value of zero. The calculation of A and TA continues for every substep of each time step until the end of the real-time hybrid simulation. The estimates of actuator delay for the adaptive compensation method are α_{es}=45 and 30 for the two actuators, respectively. The adaptive gains are both set to be k_p=0.4 and k_i=0.04.

Real-Time Hybrid Simulation Results

A total of ten ground motions recorded on stiff soil site (without near-fault effects) are selected to perform a series of real-time hybrid simulations. The ground motions are scaled to the DBE by employing the scaling procedure of Somerville [1997]. Table 2 provides the scale factors and information on these ten selected ground motions.

Table 2. Summary of ground motions for real-time hybrid simulations

Earthquake	Station	Component	Magnitude (M_w)	Distance (km)	Scale Factor
Loma Prieta 1989	Woodside	WDS000	6.93	33.87	3.62
Manjil 1990	Abbar	ABBAR--T	7.37	12.56	0.96
Manjil 1990	Abbar	ABBAR--L	7.37	12.56	1.59
Northridge 1994	LA - W 15th St	W15090	6.69	25.60	3.56
Northridge 1994	N Hollywood - Cw	CWC270	6.69	7.89	1.70
Northridge 1994	LA - Brentwood VA	0638-195	6.69	12.92	3.47
Northridge 1994	LA - Brentwood VA	0638-285	6.69	12.92	3.63
Chi-Chi 1999	TCU105	TCU105-E	7.62	17.18	2.45
Chi-Chi 1999	CHY029	CHY029-E	7.62	10.97	2.14
Chi-Chi 1999	CHY029	CHY029-N	7.62	10.97	1.56

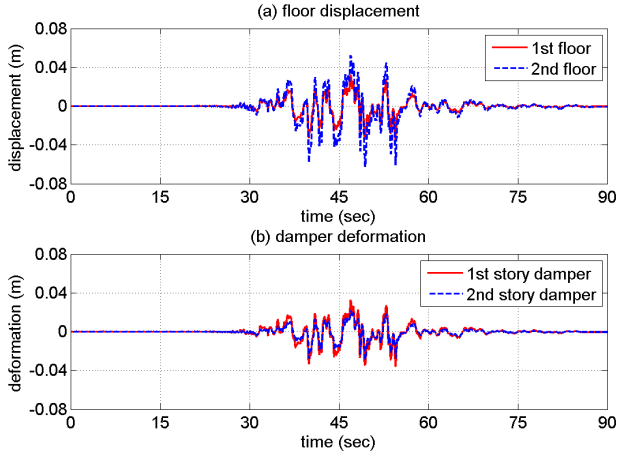

Figure 3. Real-time hybrid simulation results of MRF subjected to 1999 Chi-Chi earthquake (TCU105-E): (a) floor displacements; (b) damper deformations

The seismic performance of the MRF with MR fluid dampers is evaluated using the peak story drift and the peak residual story drift, as well as the maximum deformation of the MR fluid damper. Selected experimental results for real-time hybrid simulations using the TCU-105E component of the 1999 Chi-Chi earthquake are presented in Figs. 3 through 6. The floor displacement and damper deformation time histories are presented in Fig. 3. The MRF is observed to have a maximum lateral displacement magnitude of 35.2 mm and 62.6 mm for the first and second floors, respectively. The resulting peak story drifts are about 0.8% and 0.7% for the first and second story, respectively, which is smaller than the median story drift for all the simulations (which will be discussed later) and also smaller than the design drift of 1.7%. The residual story drifts are observed to be around zero at the end of the simulation, which means that the structure develops little, if any, inelastic response. The experimental substructures, i.e., the MR fluid dampers, developed a maximum deformation of 35.8 mm and 29.3 mm for the first and second floors, respectively. The performance of the MRF with MR fluid dampers is summarized in Table 3 for the ten different ground motions. The two components of the 1994

Northridge earthquake recorded at LA Brentwood (0638-195 and 0638-285) are observed to cause maximum story drifts around 2.6% for the first story of the MRF, which is larger than the expected performance of the design drift for the MRF. A residual story drift around 1.0% is also observed at the end of the simulations that use these two components. For the remaining eight ground motions, the MRF is observed to have achieved similar or better performance than that expected from the design procedure whereby the peak story drift is less than 1.7%. Assuming that the peak story drift response follows a lognormal distribution, the median peak story drift for all simulations is 1.09% and 1.14% for the first and second story, respectively, which is smaller than the design story drift of 1.7% used in the simplified design procedure. The median maximum damper deformation is 54 mm and 46 mm for the first and second story, respectively. The median of the residual story drifts is 0.1% and 0.07% for the first and second story, respectively, implying the expected residual drift under the DBE is small. The simplified design procedure is therefore experimentally demonstrated to be a viable method for structures with rate-dependent devices.

Table 3. Summary of real-time hybrid simulation results

Earthquake	Component	Maximum damper deformation (mm)		Peak story drift (%)		Residual story drift (%)	
		1st story	2nd story	1st story	2nd story	1st story	2nd story
Loma Prieta 1989	WDS000	36.0	31.9	0.8	0.8	0.0	0.0
Manjil 1990	ABBAR--T	51.7	47.7	1.1	1.2	0.0	0.0
Manjil 1990	ABBAR--L	43.8	37.4	0.9	0.9	0.0	0.0
Northridge 1994	W15090	43.7	39.4	0.8	1.1	0.0	0.0
Northridge 1994	CWC270	32.9	26.6	0.7	0.6	0.0	0.0
Northridge 1994	0638-195	121.7	87.7	2.6	2.3	1.0	0.7
Northridge 1994	0638-285	119.3	103.0	2.6	2.6	1.3	0.9
Chi-Chi 1999	TCU105-E	35.8	29.3	0.8	0.7	0.0	0.0
Chi-Chi 1999	CHY029-E	66.5	55.6	1.2	1.5	0.0	0.0
Chi-Chi 1999	CHY029-N	57.8	53.7	1.1	1.2	0.0	0.0

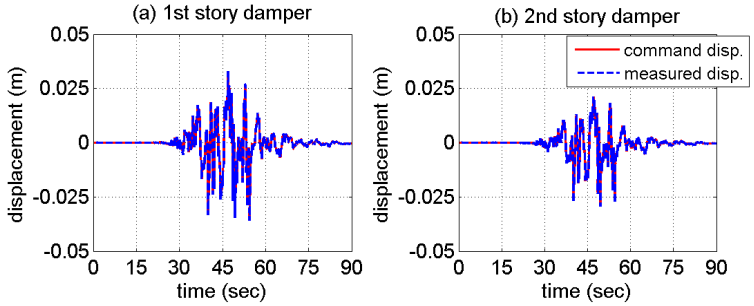

Figure 4. Comparison of command and measured actuator displacements, Chi-Chi earthquake (TCU105-E component)

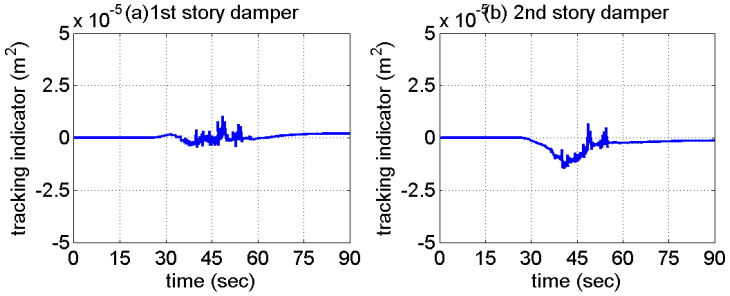

Figure 5. Time history for tracking indicator, Chi-Chi earthquake (TCU105-E component).

The actuator tracking is shown in Fig. 4 for the real-time hybrid simulation involving the 1999 Chi-Chi earthquake (TCU105-E component). The comparisons between the command and measured displacements are presented in Fig. 4(a) and 4(b) for the actuators attached to the first and second story dampers, respectively. Good agreement can be observed in the comparison, indicating that good actuators control is achieved. The time history of the tracking indicator is presented in Fig. 5(a) and 5(b) for the two actuators, where small values of the *TI* can be observed and indicates again good actuator control during the real-time hybrid simulation. The actuator tracking for all of the real-time hybrid simulations are evaluated using maximum tracking error (*MTE*), root mean square of tracking error (*RMS*), and maximum tracking indicator (*MTI*) and are summarized in Table 4. *MTE* and *RMS* are defined as

$$MTE = \max(ABS(d^c - d^m)) \tag{8a}$$

$$RMS = \sqrt{\sum_{i=1}^{N}\left[d_i^c - d_i^m\right]^2 / \sum_{i=1}^{N}\left[d_i^c\right]^2} \tag{8b}$$

It can be observed from Table 4 that the maximum value of 4.1 mm for the *MTE* occurs for the real-time hybrid simulation involving the 0638-195 component of the 1994 Northridge earthquake and corresponds to 3.38% of the 121.7 mm of maximum damper deformation developed during the simulation. The *RMS* values of the two actuators are smaller than 3.5% for all the simulations. The values for *MTI* are also observed to be small for all the simulations. These results indicate that accurate actuator tracking was achieved for all the simulations and that the experimental results are therefore considered reliable.

Table 4. Summary of actuator tracking for real-time hybrid simulation results

Earthquake	Component	*MTE* (mm)		*RMS* (%)		*MTI* (mm^2)	
		1st story	2nd story	1st story	2nd story	1st story	2nd story
Loma Prieta 1989	WDS000	1.0	1.0	1.97	1.37	19.18	15.74
Manjil 1990	ABBAR--T	2.5	1.6	3.23	2.16	54.49	40.95
Manjil 1990	ABBAR--L	2.4	1.6	3.29	2.68	29.86	18.41
Northridge 1994	W15090	2.2	1.6	2.66	1.78	25.13	51.53
Northridge 1994	CWC270	1.0	0.9	2.43	1.93	18.57	9.52
Northridge 1994	0638-195	4.1	2.2	1.16	0.50	215.08	155.10
Northridge 1994	0638-285	3.3	2.5	1.10	0.82	140.03	142.00
Chi-Chi 1999	TCU105-E	0.9	0.9	1.84	1.35	14.50	10.56
Chi-Chi 1999	CHY029-E	3.1	3.3	1.58	2.01	115.27	68.53
Chi-Chi 1999	CHY029-N	2.6	2.1	1.63	1.74	56.41	53.44

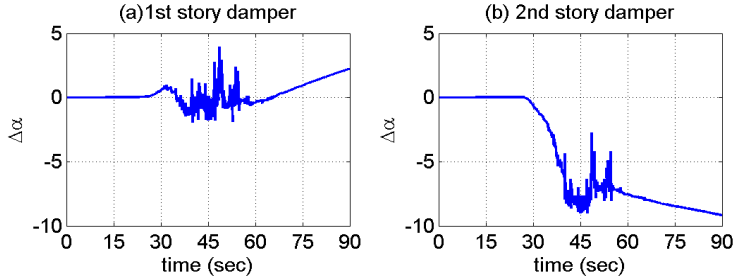

Figure 6. History for evolutionary variable Δα, Chi-Chi earthquake (TCU105-E component)

The time histories for the evolutionary variable Δα are presented in Fig. 6(a) and 6(b) for the actuators for the real-time hybrid simulation involving the 1999 Chi-Chi earthquake

(TCU105-E component). Spikes of small amplitude can be observed for the evolutionary variable $\Delta\alpha$ for both actuators, where the adaptive compensation attempts to accommodate a sudden increase in the actuator delay due to an increased deformation in the MR fluid dampers and the associated larger forces and velocities developed by the actuators. It can also be observed that the evolutionary variable $\Delta\alpha$ for the two actuators have different trends, where the actuator attached to the first story damper is observed to have a oscillation around zero while the actuator attached to the second story damper has a negative value of $\Delta\alpha$ between zero and -10. The different trends in $\Delta\alpha$ can be attributed to the different power curve capacities of the two actuators, resulting in a different delay when applying a similar force and velocity. A further inspection of $\Delta\alpha$ shows different time history for all the simulations. This can again be attributed to different demands imposed on the two actuators. Fig. 7 presents the hysteresis of the MR fluid dampers during the real-time hybrid simulation. Energy dissipation can be observed.

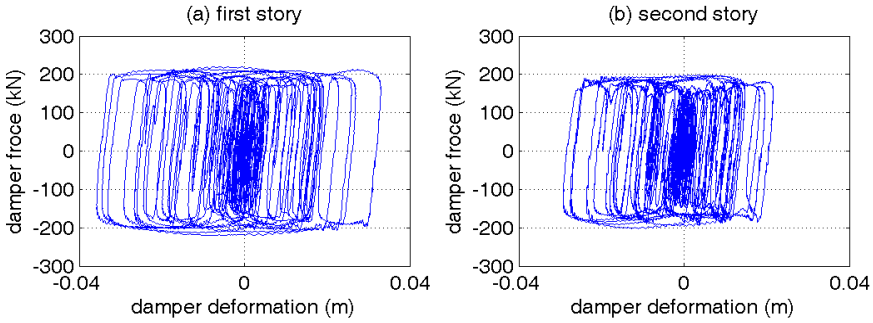

Figure 7. Hysteresis of MR dampers during the real-time hybrid simulation, Chi-Chi earthquake (TCU105-E component)

Summary and Conclusions

The performance of an MRF with MR fluid dampers in passive mode, designed using a simplified procedure, is experimentally evaluated using as series of real-time hybrid simulations. The unconditionally stable explicit CR integration algorithm and adaptive inverse compensation for actuator control is used. Statistical experimental results incorporating the ground motion variability show that a steel MRF with passive MR fluid dampers can be designed to achieve a specified performance objective involving story drift under the DBE using the simplified design procedure. The adaptive inverse compensation is experimentally demonstrated to help achieve good tracking for multiple actuators. The experimental results demonstrate the potential of the application of the real-time hybrid simulation method for evaluating design procedures and the performance of structural systems with rate-dependent devices.

Acknowledgments

This paper is based upon work supported by grants from the Pennsylvania Department of Community and Economic Development through the Pennsylvania Infrastructure Technology Alliance, and by the National Science Foundation under Grant No. CMS-0402490 within the George E. Brown, Jr. Network for Earthquake Engineering Simulation Consortium Operation. Any opinions, findings, and conclusions expressed in this paper are those of the authors and do not necessarily reflect the views of the sponsors. The MR fluid dampers used for the study presented in this paper were provided by Dr. Richard Christenson of University of Connecticut. The authors appreciate his support.

References

Bass, B.J. and Christenson, R. 2007. System identification of a 200kN Magneto-Rheological fluid damper for structural control in large-scale smart structures. *Proceedings, 2007 American Control Conference*, New York City.

Blakeborough, A., et al. 2001. The development of real-time substructure testing. *Philosophical Transactions of the Royal Society of London* A 359, 1869-1891.

Bonnet, P.A., et al. 2007. Real-time hybrid experiments with Newmark integration, MCSmd outer-loop control and multi-tasking strategies, *Earthquake Eng. and Structural Dynamics* 36(1), 119-141.

Building Seismic Safety Council (BSSC). 2003. *NEHRP recommended provisions for seismic regulations for new buildings and other structures*. *Report FEMA 450*, Federal Emergency Management Agency, Washington, D.C.

Chen, C. and Ricles, J.M. 2008a. Development of direct integration algorithms for structural dynamics using discrete control theory, *Journal of Engineering Mechanics* 134(8), 676-683.

Chen, C. and Ricles, J.M. 2008b. Stability analysis of SDOF real-time hybrid testing systems with explicit integration algorithms and actuator delay, *EQ Eng. and Structural Dynamics* 37(4), 597-613.

Chen, C., et al. 2009a. Design and Experimental Evaluation of Steel MRF with Magneto-Rheological Dampers for Seismic Hazard Mitigation, *Behaviour of Steel Structure in Seismic Areas* (STESSA), Philadelphia, PA.

Chen, C., et al. 2009b. Real-time hybrid testing using the unconditionally stable explicit integration algorithm," *Earthquake Engineering and Structural Dynamics* 38(1):23-44.

Chen, C., and Ricles, J.M. 2009. Tracking error-based servo-hydraulic actuator adaptive compensation for real-time hybrid simulation, *Journal of Structural Engineering*, in press.

Christenson, R., Lin, Y.Z., Emmons, A. and Bass, B. 2008. Large-scale experimental verification of semi-active control through real-time hybrid simulation, *Journal of Structural Eng.* 134(4), 522-534.

Darby, A.P., et al. 1999. Real-time substructure tests using hydraulic actuators, *Journal of Engineering Mechanics* 125(10):1133-11139.

Dyke S.J., Spencer B.F., Jr., Sain M.K. and Carlson J.D. 1998. An experimental study of MR dampers for seismic protection, *Smart Materials and Structures* 7(5), 693-703.

Lehigh RTMD Users Guide. 2009. http://www.nees.lehigh.edu/index.php?page=rtmd-user-s-manual.

International Code Council (ICC) 2006. *International Building Code*, Falls Church, VA.

Jansen, L.M. and Dyke, S.J. 2000. Semiactive control strategies for MR dampers: comparative study, *Journal of Engineering Mechanics* 126(8), 795-902.

Karavasilis T.L., et al. 2009. HybridFEM: A program for nonlinear dynamic time history analysis and real-time hybrid simulation of large structural systems. *ATLSS Report*, Lehigh Univ., Bethlehem, PA.

Lee, K.S. et al. 2005. Simplified design procedure for frame buildings with viscoelastic or elastomeric dampers, *Earthquake Engineering and Structural Dynamics* 34(10), 1271-1284.

Mercan, O., 2007. *Analytical and experimental studies on large scale, real-time pseudodynamic testing*. PhD. Dissertation, Department of Civil and Environmental Eng., Lehigh Univ., Bethlehem, PA.

Nakashima, M., et al. 1992. Development of real-time pseudodynamic testing, *Earthquake Engineering and Structural Dynamics* 21(1), 79-92.

Soong, T.T. and Dargush, G.F. 1997. *Passive dissipation systems in structural engineering*. John Wiley & Sons, England.

Somerville, P. 1997. *Development of ground motion time histories for Phase 2 of the FEMA/SAC Steel Project*, Report No. SAC/DB-97/04, Sacramento, CA.

Yang, G., et al. 2002, Large-scale MR fluid dampers: modeling and dynamic performance considerations, *Engineering Structures* 24(3), 309-323.

Wallace, M.I., et al. 2005, Stability analysis of real-time dynamic substructuring using delay differential equation models, *Earthquake Engineering and Structural Dynamics* 34(15), 1817-1832.